JOC Article

Density Functional Theory Study of the Intramolecular [2 + 3] Cycloaddition of Azide to Nitriles

Fahmi Himo,[†,‡] Zachary P. Demko,[§,⊥] and Louis Noodleman*[,†]

Department of Molecular Biology, TPC-15, and Department of Chemistry and The Skaggs Institute for Chemical Biology, BCC-315, The Scripps Research Institute, 10550 North Torrey Pines Road, La Jolla, California 92037

lou@scripps.edu

Received April 21, 2003

Density functional theory calculations using the hybrid functional B3LYP have been performed to study tetrazole formation by intramolecular [2 + 3] dipolar cycloaddition of organic azides and nitriles. Experimental reactivity trends are explained and rationalized in terms of a number of parameters, such as strain, tether length, and solvation and entropy effects. Interestingly, no correlation was found between the overall free energies and the free energies of activation of the reactions, due to the significant difference in strain and geometry between the transition states and products.

Introduction

Tetrazoles, an increasingly popular functionality,[1] are extraordinarily stable to both acids and bases, as well as to oxidizing and reducing conditions.[2] They provide an exceedingly robust display of functional groups at certain geometries; for example, 1-alkylated tetrazoles provide excellent isosteres for *cis*-amide bonds in peptides.[3] Thanks to these properties, tetrazoles have found wide use as metabolically stable lipophilic spacers,[4] as well as surrogates for the carboxylic acid group[5] in pharmaceuticals, not to mention in materials science.[6]

Tetrazoles can be directly synthesized via a [2 + 3] dipolar cycloaddition reaction between an azide and a nitrile. When azide salts play the role of the dipole, 1*H*-tetrazoles can be formed in high yield;[7] when organic azides are used, the 1,5-disubstituted regioisomer is observed exclusively (see Scheme 1).[1]

To date only a few highly activated nitriles are known to undergo this cycloaddition in an *inter*molecular fashion with organic azides.[8] Of course, when the azide and nitrile moieties are in the same molecule, rates of cycloaddition can be greatly enhanced, and several groups have reported the efficient synthesis of polycyclic fused tetrazoles via *intra*molecular [2 + 3] cycloaddition (see Scheme 2).[9] The scope of this reaction class has been recently expanded by Demko and Sharpless to include nitriles attached to heteroatoms (Scheme 2, Z = O, N, S).[10]

SCHEME 1. [2 + 3] Dipolar Cycloaddition of Azides and Nitriles

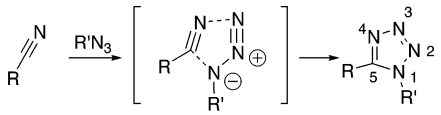

The range of the azidonitrile species which participate in these intramolecular [2 + 3] cycloadditions is quite

† Department of Molecular Biology, The Scripps Research Institute.

‡ Present address: Royal Institute of Technology, Department of Biotechnology, Theoretical Chemistry, S-106 91 Stockholm, Sweden.

§ Department of Chemistry and The Skaggs Institute for Chemical Biology, The Scripps Research Institute.

⊥ Present address: PGRD La Jolla Laboratories, Pfizer, Inc., 10777 Science Center Drive, San Diego, CA 92121.

(1) Butler, R. N. In *Comprehensive Heterocyclic Chemistry*; Katritzky, A. R., Rees, C. W., Scriven, E. F. V., Eds.; Pergammon: Oxford, U.K., 1996; Vol 4.

(2) Benson, F. R. In *Heterocyclic Compounds;* Elderfield, R. C., Ed.; John Wiley & Sons: New York, 1966; Vol 8.

(3) (a) Yu, K.-L.; Johnson, R. L. *J. Org. Chem.* **1987**, *52*, 1051. (b) Zabrocki, J.; Smith, G. D.; Dunbar, J. B., Jr.; Iijima, H.; Marshall, G. R. *J. Am. Chem. Soc.* **1988**, *110*, 5875. (c) Bartlett, P. A.; Acher, F. *Bull. Soc. Chim. Fr.* **1986**, 771.

(4) A simple search of the MDDR database (6/01) provided 173 1-alkylated and 151 2-alkylated 5-*C*-tetrazoles, and 147 1- alkylated and 33 2-alkylated 5-heterotetrazoles.

(5) Singh, H.; Chawla, A. S.; Kapoor, V. K.; Paul, D.; Malhotra, R. K. *Prog. Med. Chem.*, **1980**, *17*, 151.

(6) (a) Ostrovskii, V. A.; Pevzner, M. S.; Kofmna, T. P.; Shcherbinin, M. B.; Tselinskii, I. V. *Targets Heterocycl. Syst.* **1999**, *3*, 467. (b) Hiskey, M.; Chavez, D. E.; Naud, D. L.; Son, S. F.; Berghout, H. L.; Bome, C. A. *Proc. Int. Pyrotech. Semin.* **2000**, *27*, 3. (c) Koldobskii, G. I.; Ostrovskii, V. A. *Usp. Khim.* **1994**, *63*, 847.

(7) (a) Mihina, J. S.; Herbst, R. M. *J. Org. Chem.* **1950**, *15*, 1082. (b) Finnegan, W. G.; Henry, R. A.; Lofquist, R. *J. Am. Chem. Soc.* **1958**, *80*, 3908. (c) Wiberg, V. E.; Michaud, H. *Z. Naturforsch., Teil B* **1954**, *9*, 497. (d) Dunica, J. V.; Pierce, M. E.; Santella, J. B., III *J. Org. Chem.* **1991**, *56*, 2395. (e) Wittenberger, S. J. *Org. Prep. Proced. Int.* **1994**, *26*, 499. (f) Demko, Z. P.; Sharpless, K. B. *J. Org. Chem.* **2001**, *66*, 7945.

(8) (a) Carpenter, W. R. *J. Org. Chem.* **1962**, *27*, 2085. (b) Quast, H.; Bieber, L. *Tetrahedron Lett.* **1976**, *18*, 1485. (c) Krayushin, M. M.; Beskopylnyi, A. M.; Zlotin, S. G.; Lukyanov, O. A.; Zhulin, V. M. *Izv. Akad. Nauk. SSSR Ser. Khim.* **1980**, *11*, 2668. (d) Katner, A. S. U.S. Patent 3,962,272, 1974. (e) Demko, Z. P.; Sharpless, K. B. *Angew. Chem., Int. Ed.* **2002**, *41* (12), 2110. (f) Demko, Z. P.; Sharpless, K. B. *Angew. Chem., Int. Ed.* **2002**, *41* (12), 2113.

(9) (a) *The Chemistry of the Cyano Group*; Rappaport, Z., Ed.; Interscience Publishers: London, UK, 1970; p 351. (b) Kereszty, W. U.S. Patent 2,020,937, Nov. 12, 1935. (c) Smith, P. A. S.; Clegg, J. M.; Hall, J. H. *J. Org. Chem.* **1958**, *23*, 524. (d) Fusco, R.; Garanti, L.; Zecchi, G. *J. Org. Chem.* **1975**, *40*, 1906. (e) Garanti, L.; Zecchi, G. *J. Org. Chem.* **1980**, *45*, 4567. (f) Davis, B.; Brandstetter, T.; Smith, C.; Hackett, L.; Winchester, B. G.; Fleet, G. *Tetrahedron Lett.* **1995**, *36*, 7507. (g) Porter, T. C.; Smalley, R. K.; Teguiche, M.; Purwono, B. *Synthesis* **1997**, *7*, 773.

(10) Demko, Z. P.; Sharpless, K. B. *Org. Lett.* **2001**, *3*, 4091.

10.1021/jo030137i CCC: $25.00
Published on Web 10/23/2003

SCHEME 2. Intramolecular Cycloaddition of Azides and Nitriles

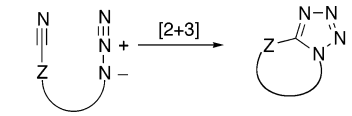

Intramolecular cycloaddition of azides and nitriles

SCHEME 3 [a]

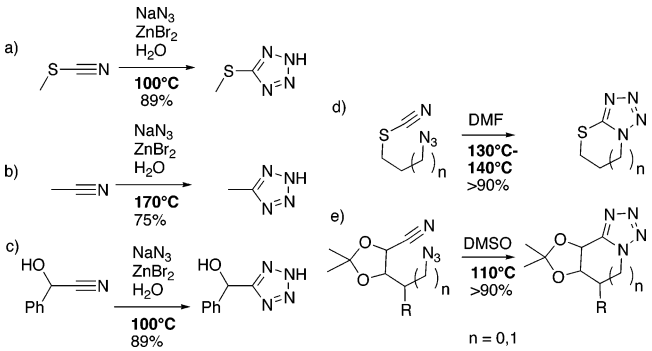

[a] Conditions: (a), (b), (c) see ref 7f; (d) see ref 10; (e) see ref 9f; R = −CH(OH)CH_2OH.

broad. The tetrazoles formed can be fused to five- or six-membered ring systems which can be either saturated or unsaturated, and the heteroatom (Scheme 2, Z) can be carbon, nitrogen, oxygen, or sulfur.

Using the temperature necessary for reaction as an approximate gauge of the activation barrier, it is possible to order the various nitriles by reactivity. For example, by examining the zinc-catalyzed transformation of various nitriles to 1*H*-tetrazoles[10] (see Scheme 3) it seems clear that thiocyanates (Scheme 3a, R−SCN) are more activated than simple alkyl nitriles (Scheme 3b, R−CN). However, examining some intramolecular cycloadditions (see Scheme 3d,e) we notice that in the cases shown, thiocyanates (Scheme 3d) seem to be less activated than the corresponding alkyl nitrile (Scheme 3e). Our initial instincts had been that the substituent on the nitrile was the main factor in the activity of the sytem; however, the seeming paradox outlined above refutes that hypothesis.

Upon closer examination, we can find other examples which demonstrate that other factors come into play. For example, in certain cases where activating groups are present at the α-position (Scheme 3c), alkyl nitriles can be as reactive as the thiocyanates. So then, what factors play the greatest role and will allow us to best predict the activation barrier of a given intramolecular cycloaddition of an azidonitrile? Is it the Thorpe−Ingold effect in a conformationally constrained system? Is it a *σ*-withdrawing substituent at the α-position? How is the substrate geometry involved?

In the present work, we have used density functional methods to study the geometries and energies of a number of intramolecular [2 + 3] dipolar cycloaddition reactions between azides and nitriles. The reactions were chosen to analyze various parameters affecting the reactivity of these compounds, such as the substitution pattern on the nitrile, tether length, strain of the resultant ring system, and conformational restraints on the backbone.

Computational Details

All geometries and energies presented in this study are computed by using the B3LYP[11] density functional theory method as implemented in the Gaussian98 program package.[12] Geometry optimizations were performed with the triple-ζ plus polarization basis set 6-311G(d,p), followed by single-point energy calculation with the larger basis set 6-311+G(2d,2p). Hessians were calculated at the B3LYP/6-311G(d,p) level of theory. Hessians provide a control that the stationary points localized are correct, with no imaginary frequencies for minima and one imaginary frequency for transition states, and also to evaluate the zero-point vibrational effects on energy, as well as to calculate the entropy contribution to the total energy.

Solvation energies were added as single-point calculations by using the conductor-like solvation model COSMO-PCM[13] at the B3LYP/6-311G(d,p) level, with the default radii of the Gaussian98 program. In this model, a cavity around the system is surrounded by polarizable dielectric continuum. The dielectric constant was chosen to the standard value for water, $\epsilon = 80$. Some of the experiments were done in DMF, which has a dielectric constant (ϵ) of 37. As the solvation energy to a first approximation is proportional to $(1 - {}^{3}/_{2\epsilon})$ for large ϵ,[14] the water and DMF values give almost identical solvation effects, especially since we are interested in reaction barriers (reactant−transition state) and relative barriers.

Results and Discussion

The azidonitrile systems studied in the present paper are displayed in Scheme 4, in which experimental temperatures and yields from literature reports of the compounds, or of closely related compounds, are indicated where appropriate.[9f,10] Reaction barriers and energies calculated with density functional theory are presented in Table 1, and the transition state structures are given in Figure 1 and in the Supporting Information. In Table 1, the energies are broken down into gas-phase energies and solvation and entropy effects to better analyze the results.

a. General Trends. First, some general observations. As seen from Table 1, the calculated barriers of the various reactions fall within a rather narrow range of energy, 28−38 kcal/mol (25−36 kcal/mol in the gas phase),[15] while the reaction energies span a slightly wider range, −5 to −17 kcal/mol (−8 to −22 kcal/mol in the gas phase). There is, furthermore, no correlation between the barriers and the free energies of reaction (see Figure 2). For example, it is interesting to note that the most exergonic reaction (reaction 9, −17.2 kcal/mol) and the

(11) (a) Becke, A. D. *Phys. Rev.* **1988**, *A38*, 3098. (b) Becke, A. D. *J. Chem. Phys.* **1993**, *98*, 1372. (c) Becke, A. D. *J. Chem. Phys.* **1993**, *98*, 5648.

(12) Frisch, M. J.; Trucks, G. W.; Schlegel, H. B.; Scuseria, G. E.; Robb, M. A.; Cheeseman, J. R.; Zakrzewski, V. G.; Montgomery, J. A., Jr.; Stratmann, R. E.; Burant, J. C.; Dapprich, S.; Millam, J. M.; Daniels, A. D.; Kudin, K. N.; Strain, M. C.; Farkas, O.; Tomasi, J.; Barone, V.; Cossi, M.; Cammi, R.; Mennucci, B.; Pomelli, C.; Adamo, C.; Clifford, S.; Ochterski, J.; Petersson, G. A.; Ayala, P. Y.; Cui, Q.; Morokuma, K.; Malick, D. K.; Rabuck, A. D.; Raghavachari, K.; Foresman, J. B.; Cioslowski, J.; Ortiz, J. V.; Baboul, A. G.; Stefanov, B. B.; Liu, G.; Liashenko, A.; Piskorz, P.; Komaromi, I.; Gomperts, R.; Martin, R. L.; Fox, D. J.; Keith, T.; Al-Laham, M. A.; Peng, C. Y.; Nanayakkara, A.; Challacombe, M.; Gill, P. M. W.; Johnson, B. G.; Chen, W.; Wong, M. W.; Andres, J. L.; Gonzalez, C.; Head-Gordon, M.; Replogle, E. S.; Pople, J. A. *Gaussian 98*, revision A.9; Gaussian, Inc.: Pittsburgh, PA, 1998.

(13) (a) Barone, V.; Cossi, M. *J. Phys. Chem.* **1998**, *102*, 1995. (b) Barone, B.; Cossi, M.; Tomasi, J. *J. Comput. Chem.* **1998**, *19*, 404.

(14) Orozco, M.; Luque, F. J. *Chem. Rev.* **2000**, *100*, 4187.

(15) To our knowledge, only one reaction of this type has been studied kinetically: Bruche, L.; Garanti, L.; Zecchi, G. *J. Chem. Res. (S)* **1983**, 202.

SCHEME 4

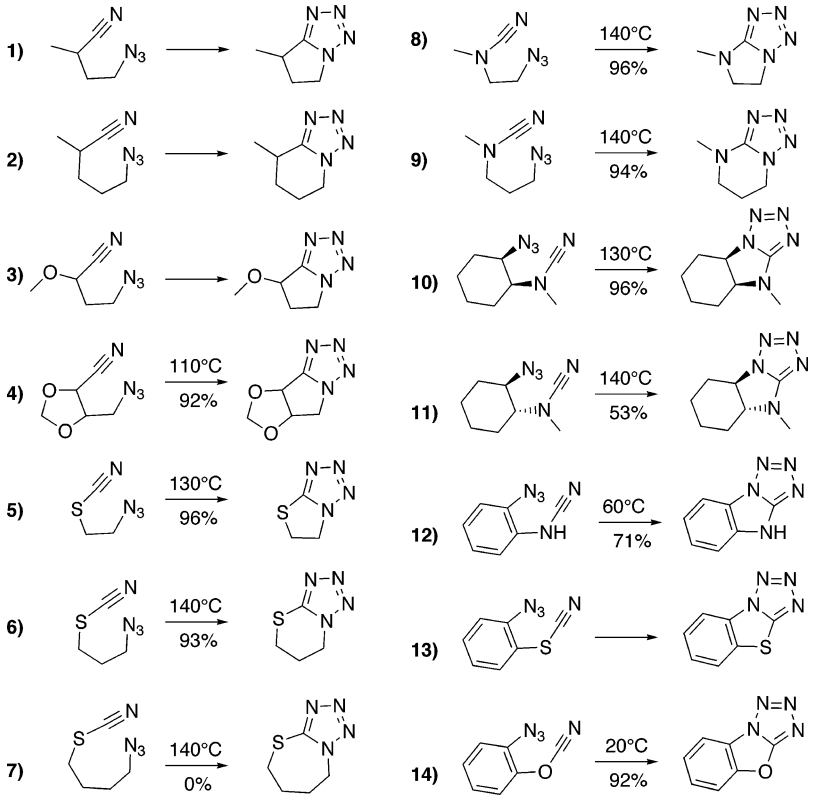

TABLE 1. Calculated Free Energy Barriers ($\Delta G^{\ddagger}$) and Reaction Free Energies (ΔG) (in kcal/mol) for Intramolecular [2 + 3] Cycloaddition Reactions[a]

	transition state				tetrazole			
reaction	gas	$\epsilon = 80$	$\Delta S^{\ddagger}$ [cal/(mol·K)]	$\Delta G^{\ddagger}$ total[b]	gas	$\epsilon = 80$	ΔS [cal/(mol·K)]	ΔG total[b]
1	+31.5	+0.6	−11.8	+36.5	−10.7	−1.7	−14.6	−7.0
2	+28.8	+1.2	−14.3	+35.3	−17.9	−2.2	−17.9	−13.5
3	+34.8	−2.1	−11.2	+36.9	−8.4	−4.7	−14.1	−7.9
4	+31.7	−3.4	−12.6	+33.0	−10.3	−6.8	−15.2	−11.4
5	+29.1	+0.1	−12.6	+33.9	−11.7	−2.8	−15.9	−8.6
6	+29.0	−0.2	−14.4	+34.2	−17.2	−4.0	−18.4	−14.3
7	+31.1	+0.4	−16.3	+37.6	−16.7	−2.7	−21.9	−11.2
8	+32.3	−0.7	−12.1	+36.1	−10.1	−3.3	−15.4	−7.6
9	+29.0	+0.7	−14.9	+35.3	−21.7	−2.3	−18.2	−17.2
10	+30.0	+0.5	−11.0	+34.5	−12.5	−1.9	−15.0	−8.8
11	+30.1	+1.8	−11.3	+36.2	−10.2	−0.9	−14.6	−5.7
12	+35.7	−2.9	−8.6	+36.0	−9.3	−5.3	−12.4	−8.6
13	+25.7	−1.3	−11.0	+28.4	−19.0	−2.3	−16.2	−15.3
14	+30.6	−2.9	−10.2	+31.5	−14.5	−3.7	−14.9	−12.7

[a] Energies are broken down into gas phase energies (gas), solvation effects using $\epsilon = 80$ ($\epsilon = 80$) and entropy effects (ΔS). [b] Entropy included at 100 °C.

least exergonic reaction (reaction 11, −5.7 kcal/mol) have very close barriers, 35.3 and 36.2 kcal/mol, respectively.

Inspection of the transition state structures of these reactions (presented in Figure 1 and the Supporting Information) shows that locally around the azide and nitrile they are quite similar. The $C_{nitrile}-N_{azide}$ bond distance, for instance, varies between 1.78 and 1.93 Å, while the $N_{nitrile}-N_{azide}$ bond distance varies between 2.13 and 2.46 Å. The similarity is even more striking when looking at some angles. The azide NNN angle varies between 132.9° and 136.5°, i.e., less than 4°, while the NCX angle of the nitrile varies between 140.4° and 150.2°. It is also worth noting that the pathways are asynchronous; we believe this is a charge effect. Previous work with azides has led us to believe that the resonance structure of azide responsible for the reactivity is that shown in Scheme 2, such that the negative charge is on the nitrogen adjacent to carbon, explaining the observed asynchrony.

As expected for this kind of addition reactions, the entropy effects are substantial, increasing the activation barriers and decreasing the free energies of the reactions. For the barriers, the entropy effect is on the order of 9−16 cal/(mol·K), and for the reaction energies it is on the order of 12−22 cal/(mol·K).

The dipole moments of the tetrazoles are in general larger than those of the reactants, resulting in a solvation stabilization of the former by up to 7 kcal/mol, as

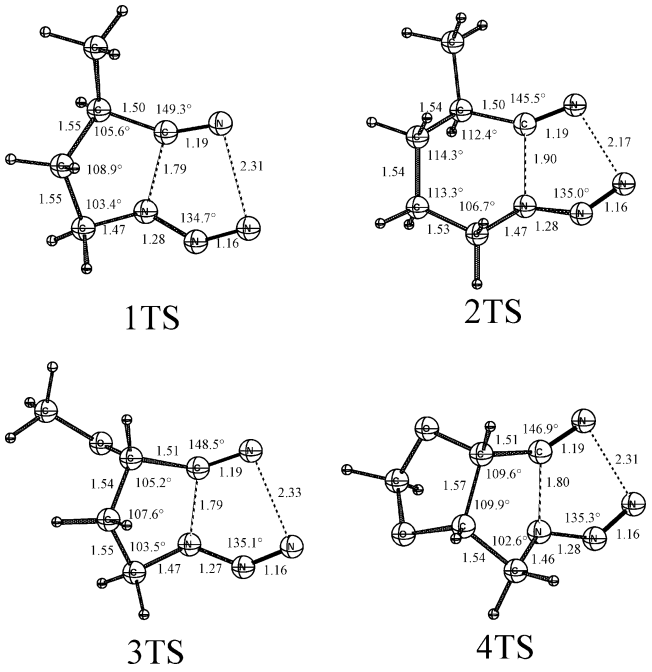

FIGURE 1. Optimized transition state structures for **1**−**4**. Bond lengths in angströms.

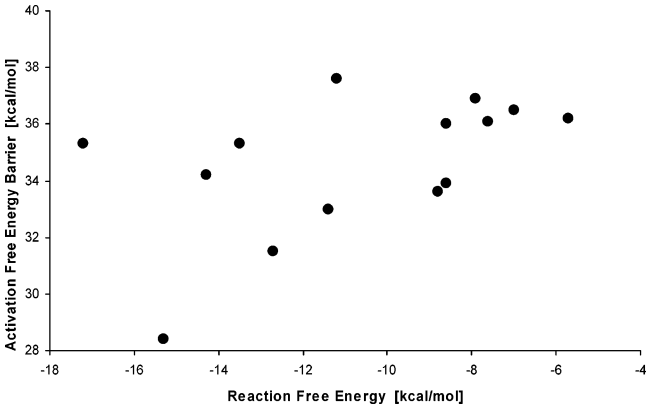

FIGURE 2. Activation free energy barriers vs reaction free energies for the intramolecular [2 + 3] cycloaddition reactions to form tetrazole.

calculated with the COSMO-PCM polarizable dielectric continuum model with $\epsilon = 80$. For transition states the solvation effects are in general smaller and can be either stabilizing or destabilizing relative to the reactants, depending on the size and nature of the substitution.

It was pointed out above that the barriers fall within the rather narrow range of energy, 28−38 kcal/mol. This energy range corresponds, however, to a reaction rate difference of 6−7 orders of magnitude, or a temperature difference of more than 100 °C. Hence, there is room for variations in reactivity for the different compounds. A discussion of some of the effects and trends contributing to the activation barrier of the reaction follows.

b. Nitrile Substitutent. Examined first is the effect of the substituent on the nitrile. Comparing reactions 1, 5, and 8, we see that the activation barriers are 36.5, 33.9, and 36.1 kcal/mol, respectively. Thus according to the calculations, nitriles attached to nitrogen (cyanamides), carbon, and sulfur (thiocyanates) have very similar barriers, with the sulfur case being a bit lower in energy. This correlates with the experimental observation that reaction 5 proceeds at a slightly lower temperature than is the case for which reaction 8 is a model.

When we look at the analogous case where an enclosed six-membered ring is created, reactions 2, 6, and 9, we see that the $\Delta G^{\ddagger}$ for the three reactions is very similar, 35.3, 34.2, and 35.3 kcal/mol, respectively. These values show that the activation is not well correlated to the electronegativity of the attached atom, since C, S, and N have electronegativities of 2.55, 2.58, and 3.04, respectively.[16] This was suprising to us in light of our previous work in which we calculated the barriers for the direct intermolecular [2 + 3] cycloaddition of methyl azide and different nitriles using the same theoretical methods.[17] There it was shown that the barrier with methyl thiocyanate is 3.1 kcal/mol lower than that for acetonitrile. Furthermore, it was seen that the reaction barriers correlate strongly with the electronegativity of the substituent.

Interestingly, when we look at reactions 12, 13, and 14, we see that the sulfur case is significantly (more than 7 kcal/mol) more active than the analogous nitrogen case. Oxygen has a higher electronegativity than sulfur, yet is less activated, though still more activated than the nitrogen case. Several effects come together to explain this trend. One relevant difference is that C–S bond lengths are longer than in the other cases. Also the sulfur atom is more flexible than first row elements and can therefore accommodate larger deviations from the ground-state geometry at lower energetic cost. In addition, sulfur can engage better in π-conjugation, which helps stabilizing the transition state involving the sulfur to a higher degree than the other substituents.

c. Tether Length. To address how much the length of the tether affects the reaction barriers, let us now examine the reactions 5, 6**,** and 7, which are identical apart from the tether length. Experimentally, when the nitrile enters as a thiocyanate (R−SCN), it was found that formation of [5,5] and [6,5] ring systems is quite favorable, while the [7,5] ring systems are not accessible under the same conditions.[10] The calculated gas-phase barriers for reactions 5, 6, and 7 are 29.1, 29.0, and 31.1 kcal/mol, respectively, while the total barriers including solvation and entropy effects are 33.9, 34.2, and 37.6 kcal/mol, respectively. This correlates very well with the experimental observations. In Table 2 we have listed selected bond angles of the reactants, transition states, and the tetrazole products of these reactions, as a measure of the amount of strain in the systems. As seen from the table, the angles of the transition state of reaction 7 deviate the most from their counterparts in the starting reactant structure, explaining in part the higher barrier for this reaction. On the other hand, the strain in the product of reaction 5 is considerably higher than in reactions 6 and 7, resulting in the lower reaction free energy of that reaction (in the gas phase −11.7 kcal/mol for reaction **5**, compared to −17.2 and −16.7 kcal/mol for reactions 6 and 7, respectively).

(16) Huheey, J. E.; Keiter, E. A.; Keiter, R. L. In *Inorganic Chemistry*, 4th ed.; HarperCollins College Publisher: New York, 1993; p 187.

(17) Himo, F.; Demko, Z. P.; Noodleman, L.; Sharpless, K. B. *J. Am. Chem. Soc.* **2002**, *124*, 12210.

TABLE 2. Selected Calculated Bond Angles for Reactions 5, 6, and 7[a]

reaction		NCS	CSC	SCC	CCN
5	reactant	175.7 (0.0)	101.7 (0.0)	114.6 (0.0)	109.1 (0.0)
	TS	144.7 (−31.0)	97.5 (−4.2)	109.0 (−5.6)	102.5 (−6.6)
	product	137.3 (−38.4)	88.7 (−13.0)	107.5 (−7.1)	103.5 (−5.6)

reaction		NCS	CSC	SCC	CCC	CCN
6	reactant	178.4 (0.0)	99.6 (0.0)	109.7 (0.0)	114.6 (0.0)	108.2 (0.0)
	TS	142.1 (−36.3)	102.3 (+2.7)	115.7 (+6.0)	113.3 (−1.3)	107.4 (−0.8)
	product	153.3 (−25.1)	98.2 (−1.4)	112.9 (+3.2)	112.4 (−2.2)	110.3 (+2.1)

reaction		NCS	CSC	SCC	CCC	CCC	CCN
7	reactant	178.5 (0.0)	99.5 (0.0)	108.6 (0.0)	113.0 (0.0)	115.0 (0.0)	108.6 (0.0)
	TS	140.4 (−38.1)	104.7 (+5.2)	117.3 (+8.7)	116.5 (+3.5)	116.0 (+1.0)	111.2 (+2.6)
	product	126.1 (−52.4)	100.5 (+1.0)	116.4 (+7.8)	116.3 (+3.3)	115.9 (+0.9)	113.9 (+5.3)

[a]The deviation from the corresponding angle in the reactant is given in parentheses.

In addition to the strain, solvation and entropy effects increase the barrier of reaction 7 further compared to reactions 5 and 6. Including these effects, the barrier for reaction 7 is 3.4 kcal/mol higher than that for reaction 6, i.e., it is 2 to 3 orders of magnitude slower. Considering that reaction 6 is run experimentally at 140 °C, the calculations predict that reaction 7 needs to be run at about 180 °C to achieve the same rate of reaction. However, above 150 °C decomposition renders the reaction futile, explaining the observation that reaction 7 is not fruitful.

Similar angle analysis can be used to explain why the [5,5] ring formations in reactions 1 and 8 have slightly higher barriers and reaction energies than their [6,5] ring counterparts in reactions 2 and 9. From this we can see that both strain and entropy play a significant role in the activation barriers.

d. Substrate Preorganization. Another factor that affects the barriers is the degree of preorganization of the reacting groups in the starting material. Mounting the dipole and dipolarophile on a rigid scaffold helps to preorganize them, and thereby lower the entropic contribution to the transition state barrier, though potentially raising the strain. For instance, the cyclohexane ring in reaction 10 helps lower the barrier by 1.6 kcal/mol compared to reaction 8 (experimentally, lowering the temperature of reaction by 10 °C). Furthermore, strain introduced by trans-ring fusion between the scaffold and the enclosed ring can affect reaction times and yields. Experimentally, the rate of formation of the product of reaction 10 is approximately 15 times that of reaction 11 at 130 °C.[10] As seen from Table 1, the calculated barrier difference in the gas phase is 0.1 kcal/mol, which increases to 1.7 kcal/mol after adding solvation and entropy effects, in excellent agreement with the measured rate difference.

Finally, reaction 4 constitutes an interesting case. It shows a considerable rate enhancement compared to reaction 1, 33.0 vs 36.5 kcal/mol. The two reactions have very similar barriers in the gas phase (31.5 and 31.7 kca/mol), and very similar entropy effects on the transition states (−11.8 and −12.6 cal/(mol·K)). The 3.5 kcal/mol difference originates almost exclusively from the solvation effect. To rule out that the effect originates from a substitution effect of the oxygen, we have calculated reaction 3, the methoxy-substituted version of reaction 1; in fact, this reaction has a higher barrier than reaction 1. The three reactions 1, 3, and 4 have very similar transition state structures (see Figure 1), with a $C_{nitrile}-N_{azide}$ bond distance of 1.79−1.80 Å and a $N_{nitrile}-N_{azide}$ bond distance of 2.31−2.33 Å.

Conclusions

In the present study we have examined the structures and energetics of a variety of intramolecular [2 + 3] dipolar cycloaddition reactions of azides and nitriles. This has been done by means of the B3LYP density functional theory method. We have argued that to reproduce experimental trends, gas-phase calculations are not sufficient. Solvation and entropy effects have to be included. In contrast to the intermolecular reactions, it was shown that the electron-withdrawing power of the substituent is not the dominant factor governing the intramolecular reactions. Effects such as strain, tether length, and preorganization play equally important roles.

Acknowledgment. We thank K. Barry. Sharpless for his advice and support (NSF CHE-9985553). F.H. thanks the Wenner-Gren Foundations for financial support. Z.D. is grateful for receiving the Skaggs Predoctoral Fellowship.

Supporting Information Available: Optimized transition state structures for reactions 5−14, and atomic coordinates and energies of all computed transition state structures. This material is available free of charge via the Internet at http://pubs.acs.org.

JO030137I